A Strongly Implicit Procedure for the Compressible Navier-Stokes Equations

Robert W. Walters*
North Carolina State University, Raleigh, North Carolina
Douglas L. Dwoyer†
NASA Langley Research Center, Hampton, Virginia
and
H. A. Hassan‡
North Carolina State University, Raleigh, North Carolina

The strongly implicit procedure of Stone is used to obtain numerical solutions of the compressible Navier-Stokes equations in conservative form. In contrast to the spatially split Douglas-Gunn type methods, the method is shown to be numerically stable for the three-dimensional wave equation. The method is applied to a variety of external and internal two-dimensional flow problems involving shock wave/boundary-layer interaction for both laminar and turbulent flows. The results are in good agreement with other methods and/or experiments.

Introduction

THE desire to simulate flows over complex and realistic configurations for a wide range of Mach numbers requires algorithms for the solution of the compressible, three-dimensional Navier-Stokes equations that are both stable and efficient. One of the primary motivations for the present work stems from the fact that the approximate-factorization (AF) schemes, such as those of Briley and McDonald[1] and Beam and Warming,[2] are unstable for the three-dimensional wave equation and for the Euler equations of gasdynamics.[3] This led to an investigation of LU methods with emphasis on the strongly implicit procedure (SIP) of Stone[4] as a way of providing both a stable and an efficient method for the solution of the compressible Navier-Stokes (CNS) equations. LU methods are those where the coefficient matrix is factored into lower and upper triangular matrices. The stability of one type of LU method for hyperbolic equations in any number of dimensions was demonstrated by Jameson and Turkel.[5] Moreover, in three dimensions, LU methods require two sweeps through the mesh as opposed to the three sweeps of an alternating-direction implicit (ADI) algorithm.

To date, LU methods have not been applied to problems requiring the solution of the CNS equations in two dimensions, such as problems involving shock wave/boundary-layer interactions. Because of this, it was felt that this investigation should concentrate on such problems and limit the three-dimensional application to a model problem.

A variety of LU methods, including those of Ref. 5, were examined in conjunction with the CNS equations. Our results indicated that although such methods may be made unconditionally stable, their convergence is slow relative to the two-dimensional Beam and Warming algorithm.[2] In an effort to determine an LU scheme that is stable in three dimensions and competitive with the Beam and Warming algorithm in two dimensions, the SIP of Stone[4] was examined. This procedure has been applied to the incompressible, two-dimensional Navier-Stokes equations in the coupled vorticity-stream function form[6] and in primitive variable form,[7] and to the CNS equations in a velocity decomposed form.[8] It has also been applied to the compressible potential equation.[9,10] The method has the major drawback of a large storage requirement arising from the recursion relationships inherent in the method.

One of the objectives of this work is to demonstrate that the SIP of Ref. 4 yields a competitive algorithm for the solution of the CNS equations in two dimensions. Another objective is to examine the performance of SIP on a model hyperbolic problem in three dimensions.

The method was applied to a number of problems involving shock wave/boundary-layer interactions for both laminar and turbulent flows. Comparisons with other methods and with experiment indicate that the method developed here is suited for calculating complex laminar and turbulent flow.

Formulation of the Problem

Governing Equations

The dimensionless strong conservation law form of the two-dimensional CNS equations in generalized coordinates can be written as

$$\frac{\partial q^*}{\partial \tau}+\frac{\partial E^*}{\partial \xi}+\frac{\partial F^*}{\partial \eta}=Re^{-1}\left(\frac{\partial R^*}{\partial \xi}+\frac{\partial S^*}{\partial \eta}\right) \tag{1}$$

where

$$q^*=q/J,\ q=[\rho,\ \rho u,\ \rho v,\ e]^t$$

$$E^*=(\xi_t q+\xi_x E+\xi_y F)/J,\quad F^*=(\eta_t q+\eta_x E+\eta_y F)/J$$

$$R^*=(\xi_x R+\xi_y S)/J,\quad S^*=(\eta_x R+\eta_y S)/J$$

$$J=\xi_x\eta_y-\xi_y\eta_x \tag{2}$$

The various quantities appearing in Eq. (2) are defined in Ref. 11. For the sake of simplicity of notation, the asterisk appearing in Eq. (1) will be dropped at this point.

Received Dec. 14, 1983; presented as Paper 84-0424 at the AIAA 22nd Aerospace Sciences Meeting, Reno, NV, Jan. 9-12, 1984; revision received Feb. 22, 1985.

*Research Assistant, Mechanical and Aerospace Engineering Department.

†Head, Computational Methods Branch, High-Speed Aerodynamics Division. Associate Fellow AIAA.

‡Professor, Mechanical and Aerospace Engineering Department. Associate Fellow AIAA.

Any quantity $G(q)^{n+1}$ can be written as

$$G(q)^{n+1} = G(q)^n + \frac{\partial G^n}{\partial q}\Delta q; \quad \Delta q = q^{n+1} - q^n \tag{3}$$

where n designates the iteration level. Using. Eq. (3) and employing either Euler or trapezoidal temporal differencing, the delta form of Eq. (1) can be written as

$$\{I + h[\delta_\xi A + \delta_\eta B - R_e^{-1}(\delta_\xi J^{-1}N + \delta_\eta J^{-1}M)]\}\Delta q$$
$$= -\Delta t[\delta_\xi E + \delta_\eta F - R_e^{-1}(\delta_\xi R + \delta_\eta S)]^n$$
$$-\alpha_e h J^{-1}[(\nabla_\xi \Delta_\xi)^2 + (\Delta_\eta \nabla_\eta)^2] J_q{}^n \tag{4}$$

where

$$A,B,M,N = \frac{\partial E}{\partial q}, \frac{\partial F}{\partial q}, \frac{\partial R}{\partial q}, \frac{\partial S}{\partial q} \tag{5}$$

and $h = \Delta t$ or $\Delta t/2$ for first- or second-order time differencing. In addition, for the convection terms, δ_ξ and δ_η are second-order central difference operators while Δ and ∇ are the one-sided forward and backward difference operators. The viscous terms are central-differenced in the usual manner.[11] The last term in Eq. (4) represents a fourth-order explicit dissipation term and is added to control the high-frequency waves associated with the difference scheme; α_e is an explicit smoothing parameter.

If implicit smoothing terms are used, they are added to the left-hand side of Eq. (4) in the form

$$-\alpha_1 h J^{-1}(\nabla_\xi \Delta_\xi + \nabla_\eta \Delta_\eta) J \Delta q \tag{6}$$

where α_i is an implicit smoothing parameter. Note that the implicit smoothing terms do not affect the steady-state accuracy of the results. On the other hand, the explicit smoothing terms are of higher order and, as such, do not affect the formal accuracy of the method.

The three-dimensional linear wave equation considered here had the form

$$\frac{\partial u}{\partial t} + a\frac{\partial u}{\partial x} + b\frac{\partial u}{\partial y} + c\frac{\partial u}{\partial z} = 0 \tag{7}$$

where a, b, and c are scalar coefficients. The particular coefficients and the boundary conditions employed are given in Ref. 3.

Method of Solution

The finite difference representation of Eq. (4) can be written as

$$a_{j,k}\Delta q_{j,k-1} + b_{j,k}\Delta q_{j-1,k} + c_{j,k}\Delta q_{j,k}$$
$$+ d_{j,k}\Delta q_{j+1,k} + e_{j,k}\Delta q_{j,k+1} = \tilde{R}_{j,k} \tag{8}$$

where j and k denote spatial indices, $a,b,c,d,$ and e are 4×4 matrices, and $\tilde{R}$ represents the complete right-hand side of Eq. (4). It should be pointed out that five-point molecules, such as the one indicated in Eq. (8), can be arrived at by other forms of discretization. As an example, flux-vector splitting with appropriate one-sided differencing would yield the same molecule. The use of first-order differencing to generate the left-hand side of Eq. (8) does not preclude the use of second-order one-sided differencing to generate the right-hand side of Eq. (8) and thus maintain the second-order accuracy of the solution. All results presented here are based on central differencing.

For convenience in describing the SIP, Eq. (8) can be written in matrix notation as

$$Q\Delta q = \tilde{R} \tag{9}$$

It is well known that for large sets of equations, an exact decomposition of Q is not efficient. In the strongly implicit procedure, one seeks an approximate decomposition of Q such that

$$Q \approx \mathrm{LU} \tag{10}$$

where the LU matrices are sparse lower and upper triangular matrices, respectively. Substitution of Eq. (10) into Eq. (9) results in

$$[\mathrm{LU}]\Delta q = \tilde{R} \tag{11}$$

which is implemented by the sequence

$$\mathrm{LV} = \tilde{R} \tag{12}$$

$$U\Delta q = V \tag{13}$$

$$q^{n+1} = q^n + \Delta q \tag{14}$$

The elements of the L and U matrices are given in Appendix A.

Storage Requirements

As may be seen from Appendix A, for the general case where $\alpha \neq 0$, one would have to store the large arrays $\hat{d}_{j,k}$ and $\hat{e}_{j,k}$. Each of these arrays have the dimension $(J,K,4,4)$, where J and K represent the number of interior mesh points in each coordinate direction. Thus, these two arrays require 8 times the storage of the dependent variables Δq. In three dimensions, one has three large arrays of dimension $(I,J,K,5,5)$ and, consequently, require 15 times the storage of the dependent variables.

For the special case where $\alpha = 0$, Eq. (Al) can be multiplied by $\hat{c}_{j,k}$ to yield

$$\hat{c}_{j,k}\Delta q_{j,k} + d_{j,k}\Delta q_{j+1,k} + e_{j,k}\Delta q_{j,k+1} = \hat{c}_{j,k}V_{j,k} \tag{15}$$

This eliminates the need of storing two large arrays since $d_{j,k}$ and $e_{j,k}$ are known. Thus, only $\hat{c}_{j,k}$ needs to be stored. The same is true in three-dimensions, i.e., only one large array needs to be stored instead of three.

Boundary Conditions

At the wall, a no-slip condition is employed, together with the requirement that the normal derivative of the pressure is zero. Most of the results presented here assumed adiabatic wall conditions. Thus,

$$u = v = 0, \quad \frac{\partial p}{\partial n} = \frac{\partial T}{\partial n} = 0 \text{ at a wall} \tag{16}$$

when n indicates the normal direction. Note that the last two conditions imply, for a perfect gas, that $\partial\rho/\partial n = 0$ at the wall.

When the flow conditions at the upstream boundary are supersonic, one sets

$$\Delta q = 0 \tag{17}$$

On the other hand, for subsonic conditions at the upstream boundary (for the problems considered here), P_0 and T_0 are assumed given, $v = 0$, and the pressure is determined by extrapolation. For subsonic conditions at the downstream boundary, the pressure is assumed given and the remaining

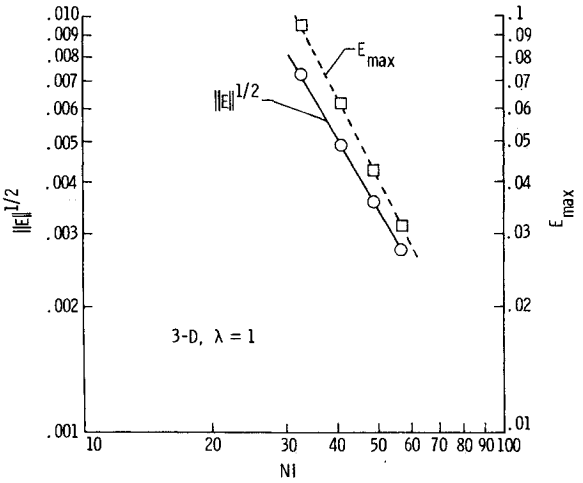

Fig. 1 Spatial convergence of SIP for the three-dimensional wave equation.

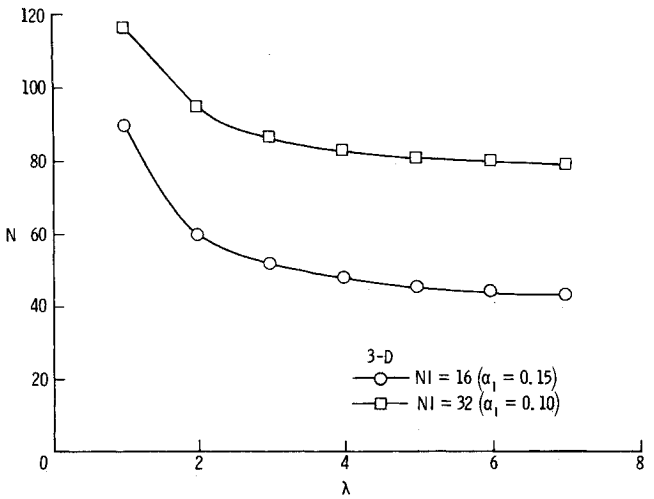

Fig. 2 Effect of Courant number on convergence of SIP for the three-dimensional wave equation.

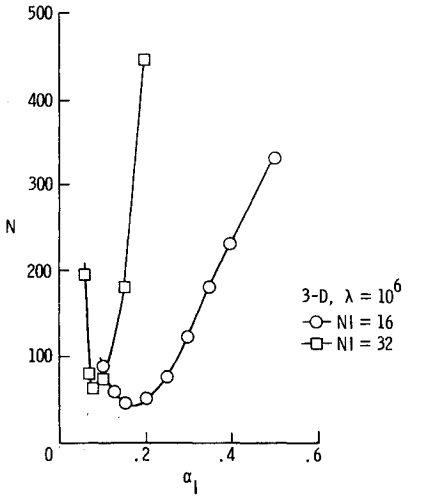

Fig. 3 Effect of implicit smoothing parameter on convergence of SIP for the three-dimensional wave equation.

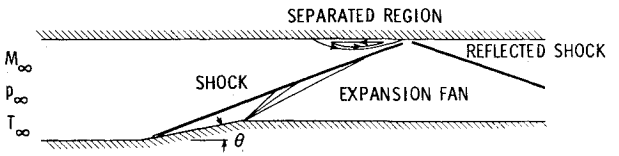

Fig. 4 Sketch of supersonic inlet problem.

flow properties are determined by extrapolation. Extrapolation is employed when supersonic conditions exist at the downstream boundary.

All boundary conditions employed here are implemented implicitly. The simplest procedure for such implementation is to cast each boundary condition in delta form similar to that given by Eq. (8). The advantage of casting the boundary conditions in a form that does not involve more than three points in any given direction is that it leaves the interior point scheme unaltered.

Results and Discussion

The algorithms developed here have been applied to model problems and a variety of fluid flow problems for both laminar and turbulent flows. Only a few representative results will be presented here. Because methods that discretize the residual in an identical manner converge to the same steady-state solution, if one exists, then their relative efficiencies can be determined from an examination of their respective convergence histories. In all problems, the efficiency of the method in converging the problem to steady state was examined in comparison with the method of Beam and Warming.[2] Numerical experience of applying the general form of SIP, as described in Appendix A, to predominantly hyperbolic equations indicates that the convergence rate is almost independent of the value of α. For the two-dimensional applications, the performance of SIP with $\alpha=0$ (hereafter referred to solely as SIP) was quite similar to the Beam and Warming method.

Since one major potential application of LU methods is in three dimensions, the solution to the three-dimensional, steady, wave equation was examined. The details of the problem are given in Ref. 3. Figure 1 shows the results of applying the SIP on a sequence of grids (*NI* is the number of mesh intervals in one direction). The accuracy of the solution was measured by computing the maximum error and the L_2-norm of the error between the exact and numerical solutions. The slope of the maximum error is approximately two, indicating second-order accuracy. Figure 2 shows the dependence of the SIP convergence rate on the Courant number, $\lambda=\Delta t/\Delta x$. For large Courant numbers, the number of iterations required to reduce the L_2-norm of the error to a fixed tolerance, ϵ (i.e., $\|E^n\|_2/\|E^0\|_2<\epsilon$) becomes a constant independent of λ. This has been observed for Courant numbers as large as 10^6. However, for $\lambda>2$, some form of implicit damping is required. The effect of the implicit smoothing parameter α_i on the convergence rate is shown in Fig. 3. As can be seen, the iterative convergence rate of the method is very sensitive to α_i although the steady solution is independent of this parameter.

In order to evaluate the iterative performance of SIP in fluid flow applications, several test problems have been studied. Results for two of these problems will be discussed. The first is the supersonic internal flow problem described in Ref. 12, which involves shock and expansion waves and their interaction with each other and with the boundary layer, resulting in the formation of separation bubbles. The geometry considered is shown in Fig. 4. Figures 5 and 6 show the convergence histories of the total and steady residuals for SIP compared to the Beam and Warming method. The total residual is taken to be an L_2-norm of the right-hand side of Eq. (4). This residual contains contributions from both the steady-state terms and the explicitly added fourth-order damping terms and thus is a measure of how Δq tends to zero. The steady-state residual contains only the terms that satisfy the discretized version of the steady governing equations. An examination of the figures indicates

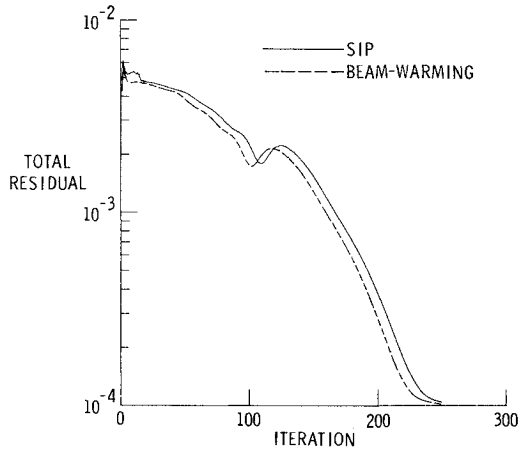

Fig. 5 Comparison of convergence histories (total residual).

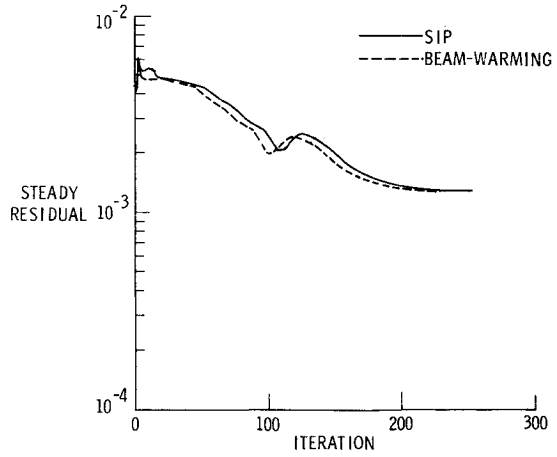

Fig. 6 Comparison of convergence histories (steady residual).

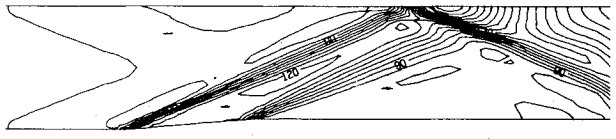

Fig. 7 Pressure contours for a 5-deg wedge angle with an entrance Mach number of 3.

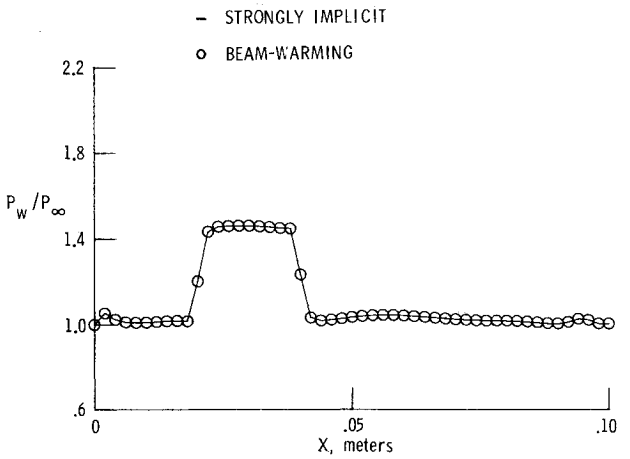

Fig. 8 Lower wall pressure distribution (5-deg wedge angle).

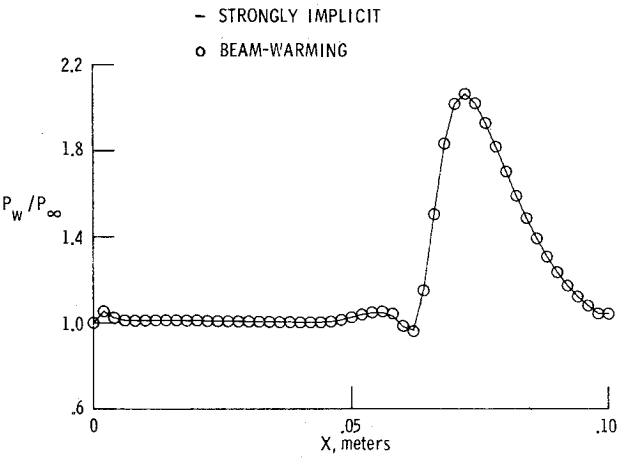

Fig. 9 Upper wall pressure distribution (5-deg wedge angle).

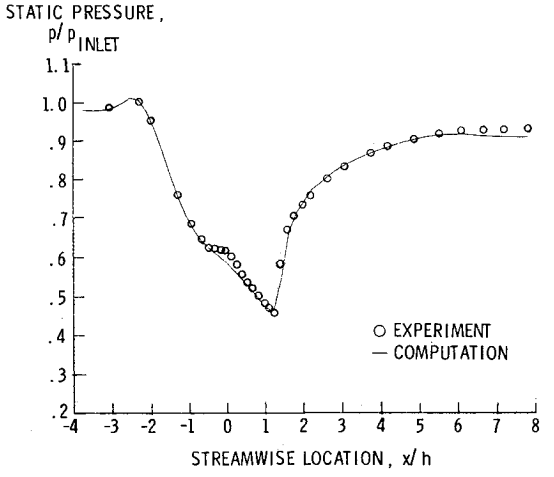

Fig. 10 Experimental and predicted pressure distribution along the top wall of the diffuser.

that the methods have similar convergence histories. For both methods, the total residual continues to decrease with continuing iteration while the true steady-state residual flattens out. The difference between the two residuals thus represents the magnitude of the smoothing terms. Figure 7 shows the pressure contours for the 5-deg wedge and an entrance Mach number of 3, while Figs. 8 and 9 present pressure distributions for the lower and upper surfaces. All of the results are qualitatively correct and, as expected, compare well with the Beam and Warming method.

The second problem involves the simulation of a compressible, turbulent flow in the terminal shock region of an inlet/diffuser. Experimental measurements are given in Ref. 13, while Ref. 14 presents the results of a numerical simulation using an AF method. The calculation presented here differs from that of Ref. 14 in a number of ways. In addition to the different algorithm and inlet boundary conditions, the algebraic eddy viscosity model of Baldwin and Lomax[15] and a complete differential energy equation are used here. Finally, in this study, a simple grid was used that contained 61 equally spaced mesh points in the streamwise direction and 31 points, which were clustered near both walls, in the transverse direction.

The top and bottom wall pressure distributions are compared with the experimental data in Figs. 10 and 11. The numerical results are seen to compare favorably with the experiment. Mach number contours and dimensionless static pressure contours are displayed in Figs. 12 and 13, respectively. The results are indicative of the flow phenomenon one expects to observe for this type of problem and are in good agreement with the results of Ref. 14.

There is reason to believe that for this type of problem, cycling α may improve convergence. However, convergence

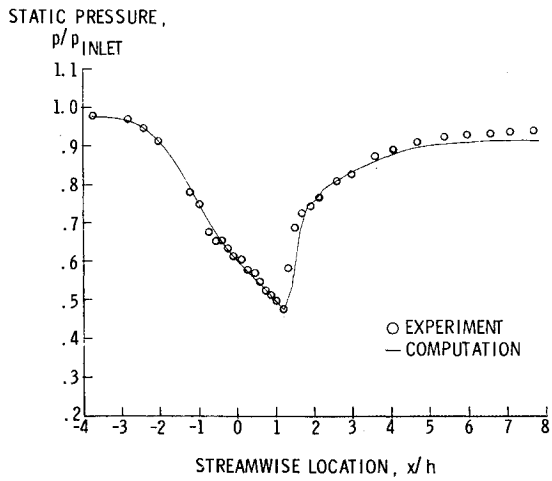

Fig. 11 Experimental and predicted pressure distribution along the bottom wall of the diffuser.

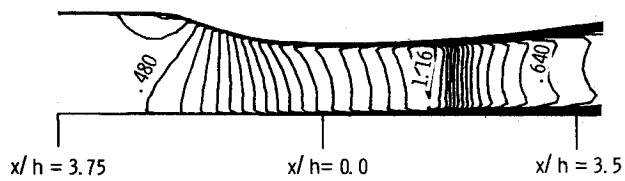

Fig. 12 Mach number contours.

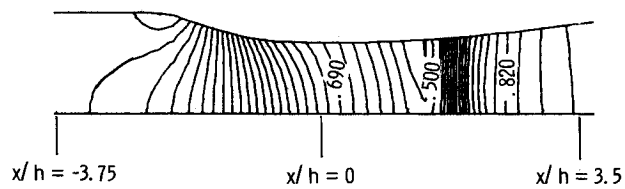

Fig. 13 Dimensionless static pressure contours.

histories show that this is not the case. Moreover, the rate of convergence for problems using the complete Navier-Stokes equations did not show any significant dependence on α_i, the implicit damping coefficient, for the range examined.

The computational time per iteration of the SIP and Beam and Warming algorithms are approximately equal. In particular, for the general case of SIP, 16% more CPU time per iteration was required than for the Beam-Warming algorithm, and for the special case of $\alpha=0$, the increase was merely 8%. According to Ref. 16, SIP has been found to converge in fewer iterations than AF for most problems tested. Consequently, for the range of problems examined, it can be stated that the total CPU time required to achieve a fixed tolerance is about the same for the two methods.

The maximum Courant numbers for the flow problems that have been studied range from 150 for the well-known shock wave/boundary-layer interaction problem[2] to approximately 50 for the terminal shock problem.

Concluding Remarks

The class of problems in which shock wave/boundary-layer interactions are the dominant flow phenomenon require the solution of the compressible Navier-Stokes equations. Our experience with the strongly implicit procedure suggests that it is a viable method for the solution of these problems and others involving separated flows. Although the applications to three dimensions were limited to the wave equation, it is felt that the method has potential for analyzing complex three-dimensional flows.

Acknowledgment

The authors would like to acknowledge many helpful discussions with Drs. Ajay Kumar and Julius E. Harris, of the Computational Methods Branch of the NASA Langley Research Center, and Dr. Stephen Davis, of ICASE. This paper was supported in part by NASA Grant NAG1-244.

Appendix A: Derivation of SIP in Two Dimensions

The recursion relations associated with the general form of the strongly implicit procedure applied to Eq. (8) can be obtained as follows. One seeks a solution to Eq. (8) in the form

$$\Delta q_{j,k}+\hat{d}_{j,k}\Delta q_{j+1,k}+\hat{e}_{j,k}\Delta q_{j,k+1}=V_{j,k} \tag{A1}$$

Writing Eq. (A1) at $j-1,k$ and $j,k-1$ yields

$$\Delta q_{j-1,k}=V_{j-1,k}-\hat{d}_{j-1,k}\Delta q_{j,k}-\hat{e}_{j-1,k}\Delta q_{j-1,k+1} \tag{A2}$$

$$\Delta q_{j,k-1}=V_{j,k-1}-\hat{d}_{j,k-1}\Delta q_{j+1,k-1}-\hat{e}_{j,k-1}\Delta q_{j,k} \tag{A3}$$

If one substitutes Eq. (A2) and (A3) into Eq. (8), additional contributions to the solution at the mesh point j,k, will appear from the $j-1$, $k+1$ and $j+1$, $k-1$ mesh points. In order to account partially for these additional contributions, Stone[5] suggests approximating their influence in terms of the dependent variables at the five mesh locations in Eq. (8) with the result

$$\Delta q_{j+1,k-1}\simeq\alpha(-\Delta q_{j,k}+\Delta q_{j+1,k}+\Delta q_{j,k-1}) \tag{A4}$$

and

$$\Delta q_{j-1,k+1}\simeq\alpha(-\Delta q_{j,k}+\Delta q_{j-1,k}+\Delta q_{j,k+1}) \tag{A5}$$

where α is an iteration parameter in the range [0,1]. The left-hand side is modified to account for these terms. One obtains

$$\begin{aligned}&a_{j,k}\Delta q_{j,k-1}+b_{j,k}\Delta q_{j-1,k}+c_{j,k}\Delta q_{j,k}\\&\quad+\mathrm{d}_{j,k}\Delta q_{j+1,k}+e_{j,k}\Delta q_{j,k+1}+f_{j,k}[\Delta q_{j+1,k-1}\\&\quad-\alpha(-\Delta q_{j,k}+\Delta q_{j+1,k}+\Delta q_{j,k-1})]+g_{j,k}\\&\quad\times[\Delta q_{j-1,k+1}-\alpha(-\Delta q_{j,k}+\Delta q_{j-1,k}+\Delta q_{j,k+1})]=\tilde{R}_{j,k}\end{aligned} \tag{A6}$$

where $f_{j,k}$ and $g_{j,k}$ will be determined from the decomposition. It should be noted that Eq. (A6) is the equation that is actually solved by LU decomposition instead of Eq. (8). Substituting Eq. (A2) and (A3) into Eq. (A6) and equating coefficients with Eq. (A1) yields

$$f_{j,k}=\hat{a}_{j,k}\hat{d}_{j,k-1} \tag{A7}$$

$$g_{j,k}=\hat{b}_{j,k}\hat{e}_{j-1,k} \tag{A8}$$

$$\hat{a}_{j,k}=a_{j,k}-\alpha f_{j,k} \tag{A9}$$

$$\hat{b}_{j,k}=b_{j,k}-\alpha g_{j,k} \tag{A10}$$

$$\hat{c}_{j,k}=c_{j,k}+\alpha(f_{j,k}+g_{j,k})-\hat{a}_{j,k}\hat{e}_{j,k-1}-\hat{b}_{j,k}\hat{d}_{j-1,k} \tag{A11}$$

$$\hat{d}_{j,k}=\hat{c}_{j,k}^{-1}(d_{j,k}-\alpha f_{j,k}) \tag{A12}$$

$$\hat{e}_{j,k}=\hat{c}_{j,k}^{-1}(e_{j,k}-\alpha g_{j,k}) \tag{A13}$$

$$V_{j,k}=\hat{c}_{j,k}^{-1}(\tilde{R}_{j,k}-\hat{a}_{j,k}V_{j,k-1}-\hat{b}_{j,k}V_{j-1,k}) \tag{A14}$$

Equations (A1) and (A7)-(A14) are the relations needed to implement the strongly implicit procedure in its general form.

Appendix B: Stability Analysis of SIP for the Three-Dimensional Wave Equation

Application of linear stability theory requires the LU decomposition to yield an upper triangular matrix whose diagonal coefficients vary smoothly in space. To show this, one can begin by seeking a matrix decomposition that yields a constant coefficient upper triangular matrix and then determine if this particular matrix factorization is stable in terms of propagation of roundoff errors in space.

Central differencing of the wave equation

$$\frac{\partial u}{\partial t}+a\frac{\partial u}{\partial x}+b\frac{\partial u}{\partial y}+c\frac{\partial u}{\partial z}=0 \tag{B1}$$

yields

$$\Delta u_{\ell,j,k}+\lambda(\Delta u_{\ell+1,j,k}+\Delta u_{\ell,j+1,k}+\Delta u_{\ell,j,k+1}-\Delta u_{\ell-1,j,k}-\Delta u_{\ell,j-1,k}-\Delta u_{\ell,j,k-1})=-\lambda(u_{\ell+1,j,k}+u_{\ell,j+1,k}+u_{\ell,j,k+1}-u_{\ell-1,j,k}-u_{\ell,j-1,k}-u_{\ell,j,k-1})\equiv R_{\ell,j,k} \tag{B2}$$

where, without loss of generality,

$$\lambda=\frac{a\Delta t}{\Delta x}=\frac{b\Delta t}{\Delta y}=\frac{c\Delta t}{\Delta z} \tag{B3}$$

A solution of Eq. (B2) is sought in the form

$$\beta_{\ell,j,k}\Delta u_{\ell,j,k}+\lambda(\Delta u_{\ell+1,j,k}+\Delta u_{\ell,j+1,k}+\Delta u_{\ell,j,k+1})=V_{\ell,j,k} \tag{B4}$$

Substituting Eq. (B4) into Eq. (B2) and setting $\alpha=0$, one finds

$$[1+\lambda^2(\beta^{-1}_{\ell-1,j,k}+\beta^{-1}_{\ell,j-1,k}+\beta^{-1}_{\ell,j,k-1})]\Delta u_{\ell,j,k}+\lambda(\Delta u_{\ell+1,j,k}+\Delta u_{\ell,j+1,k}+\Delta u_{\ell,j,k+1})=R_{\ell,j,k}+\lambda(V_{\ell-1,j,k}\beta^{-1}_{\ell-1,j,k}+V_{\ell,j-1,k}\beta^{-1}_{\ell,j-1,k}+V_{\ell,j,k-1}\beta^{-1}_{\ell,j,k-1}) \tag{B5}$$

Comparing Eq. (B4) and (B5), one finds

$$\beta_{\ell,j,k}=1+\lambda^2(\beta^{-1}_{\ell-1,j,k}+\beta^{-1}_{\ell,j-1,k}+\beta^{-1}_{\ell,j,k-1}) \tag{B6}$$

$$V_{\ell,j,k}=R_{\ell,j,k}+\lambda(V_{\ell-1,j,k}\beta^{-1}_{\ell-1,j,k}+V_{\ell,j-1,k}\beta^{-1}_{\ell,j-1,k}+V_{\ell,j,k-1}\beta^{-1}_{\ell,j,k-1}) \tag{B7}$$

The upper triangular matrix has constant coefficients on the off-diagonals. For the case where $\beta_{\ell,j,k}=\beta$, Eq. (B6) yields

$$\beta^2-\beta-3\lambda^2=0 \tag{B8}$$

which has the solution

$$\beta_{\pm}=[1\pm(1+12\lambda^2)^{1/2}]/2 \tag{B9}$$

In order to determine the propagation of roundoff error in space, Eq. (B6) can be written as

$$\beta_{\ell,j,k}=1+\frac{\beta(\beta-1)}{3}[\beta^{-1}_{\ell-1,j,k}+\beta^{-1}_{\ell,j-1,k}+\beta^{-1}_{\ell,j,k-1}] \tag{B10}$$

Setting

$$\beta_{\ell,j,k}=\beta+\epsilon_{\ell,j,k},\text{etc.} \tag{B11}$$

substituting into Eq. (B10), and neglecting terms of order ϵ^2 and higher, one finds

$$\epsilon_{\ell,j,k}=(\epsilon_{\ell-1,j,k}+\epsilon_{\ell,j-1,k}+\epsilon_{\ell,j,k-1})(1-\beta)/(3\beta) \tag{B12}$$

As is seen from Eq. (B12), in order to prevent roundoff error from growing from point to point,

$$|(1-\beta)/3\beta|<1 \tag{B13}$$

Using Eq. (B9), one can see that the above inequality holds for any λ using the β_+ solution and does not hold using the β_- solution. Thus, there is a $\beta=$constant solution (the β^+ root), which results in the decay of the error.

The temporal stability of SIP can now be addressed for the case where $\beta=$constant. According to the von Neumann stability analysis, one assumes

$$u_{\ell,j,k}=\xi^n\exp[i(\gamma_\ell x+\gamma_j y+\gamma_k z)] \tag{B14}$$

$$V_{\ell,j,k}=\eta^n\exp[i(\gamma_\ell x+\gamma_j y+\gamma_k z)] \tag{B15}$$

Substituting Eqs. (B14) and (B15) into Eq. (B7) and using the definition of $R_{\ell,j,k}$ yields

$$(\eta/\xi)^n=-\beta(\nu-\bar{\nu})/(\beta-\bar{\nu}) \tag{B16}$$

where

$$\nu=\lambda(e^{i\theta_x}+e^{i\theta_y}+e^{i\theta_z}),\ \theta_x=\gamma_\ell\Delta x,\text{ etc.} \tag{B17}$$

and $\bar{\nu}$ is the complex conjugate of ν. Similarly, substituting Eqs. (B15) and (B16) into Eq. (B4) and using Eq. (B17) gives

$$G=\xi^{n+1}/\xi^n=(\beta^2-\nu\bar{\nu})/[(\beta^2-\nu\bar{\nu}+\beta(\nu-\bar{\nu})] \tag{B18}$$

Because $\nu\bar{\nu}$ is real, $|G|<1$ always.

If stability problems arise in this method, the source is likely to be the growth of the error due to the repeated application of the recursion relations as one moves from one point to another. In this case, the addition of implicit dissipation will stabilize the scheme. This is supported by the numerical results obtained here. As was pointed out earlier, implicit dissipation was required to stabilize the solution of the wave equation for Courant numbers greater than 2. This may be contrasted with the fact that for the same test problem and the same temporal advancement scheme, the spatially split schemes will not yield a solution at moderate to high Courant numbers for any amount of implicit dissipation.

References

[1]Briley, W. R. and McDonald, H., "Solution of the Multidimensional Compressible Navier-Stokes Equations by the Generalized Implicit Method," *Journal of Computational Physics,* Vol. 24, Aug. 1977, pp. 372-397.

[2]Beam, R. M. and Warming, R. F., "An Implicit Factored Scheme for the Compressible Navier-Stokes Equations," *AIAA Journal,* Vol. 16, April 1978, pp. 393-402.

[3]Abarbanel, S. S., Dwoyer, D. L., and Gottlieb, D., "Stable Implicit Finite-Difference Methods for Three-Dimensional Hyperbolic Systems," ICASE Rept. 82-39, Nov. 1982.

[4]Stone, H. L., "Iterative Solution of Implicit Approximations of Multidimensional Partial Differential Equations," *SIAM Journal of Numerical Analysis,* Vol. 5, Sept. 1968, pp. 530-558.

[5]Jameson, A. and Turkel, E., "Implicit Schemes and LU Decompositions," *Mathematics of Computation*, Vol. 37, Oct. 1981, pp. 385-397.

[6]Rubin, S. G. and Khosla, P. K., "Navier-Stokes Calculations with a Coupled Strongly Implicit Method, Part 1: Finite-Difference Solutions," AIAA Paper 79-0011, Jan. 1979.

[7]Zedan, M. and Schneider, G. E., "A Strongly Implicit Simultaneous Variable Solution Procedure for Velocity and Pressure in Fluid Flow Problems," AIAA Paper 83-1569, June 1983.

[8]Swanson, R. C., Rubin, S. G., and Khosla, P. K., "Calculation of Afterbody Flows with a Composite Velocity Formulation," AIAA Paper 83-1736, July 1983.

[9]Sankar, N. L., "A Multigrid Strongly Implicit Procedure for Two-Dimensional Transonic Potential Flow Problems," AIAA Paper 82-0931, June 1982.

[10]Sankar, N. L., Malone, J. B., and Tassa, Y., "A Strongly Implicit Procedure for Steady Three-Dimensional Transonic Potential Flows," *AIAA Journal*, Vol. 20, May 1982, pp. 598-605.

[11]Steger, J. L., "Implicit Finite-Difference Simulation of Flow About Arbitrary Two-Dimensional Geometries," *AIAA Journal*, Vol. 16, July 1978, pp. 679-686.

[12]Kumar, A., "Some Observations on a New Numerical Method for Solving the Navier-Stokes Equations," NASA TP-1934, Nov. 1981.

[13]Bogar, T. J., Sajben, M., and Kroutil, J. C., "Characteristic Frequency and Length Scales in Transonic Diffuser Flow Oscillations," AIAA Paper 81-1291, 1981.

[14]Liu, N. S., Shamroth, S. J., and McDonald, H., "Numerical Solution of the Navier-Stokes Equations for Compressible, Turbulent Two/Three Dimensional Flows in the Terminal Shock Region on an Inlet/Diffuser," AIAA Paper 83-1892, July 1983.

[15]Baldwin, B. S. and Lomax, H., "Thin Layer Approximation and Algebraic Model for Separated Turbulent Flows," AIAA Paper 78-257, Jan. 1978.

[16]Walters, R. W., "LU Methods for the Compressible Navier-Stokes Equations," Ph.D. Thesis, North Carolina State University, Raleigh, April 1984.